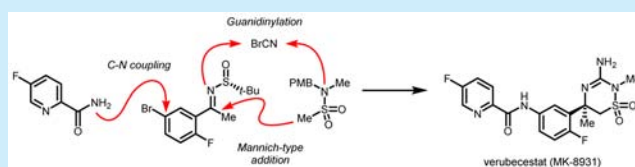


Synthesis of Verubecestat, a BACE1 Inhibitor for the Treatment of Alzheimer's Disease

David A. Thaisrivongs,^{*,†} Steven P. Miller,^{*,†} Carmela Molinaro,[†] Qinghao Chen,[†] Zhiguo J. Song,[†] Lushi Tan,[†] Lu Chen,[§] Wenyong Chen,[†] Azzeddine Lekhal,[‡] Sarah K. Pulicare,[‡] and Yanke Xu[‡][†]Process Chemistry and [‡]Chemical Engineering Research and Development, Process Research and Development, Merck Research Laboratories, P.O. Box 2000, Rahway, New Jersey 07065, United States,[§]WuXi AppTec (Shanghai) Pharmaceutical Co., Ltd., 288 Fute Zhong Road, Waigaoqiao Free Trade Zone, Shanghai 200131, China

S Supporting Information

ABSTRACT: Verubecestat is an inhibitor of β -secretase being evaluated for the treatment of Alzheimer's disease. The first-generation route relies on an amide coupling with a functionalized aniline, the preparation of which introduces synthetic inefficiencies. The second-generation route replaces this with a copper-catalyzed C–N coupling, allowing for more direct access to the target. Other features of the new route include a diastereoselective Mannich-type addition into an Ellman sulfinyl ketimine and a late-stage guanidinylation.



A recent World Health Organization (WHO) report estimates that in 2010, 35.6 million people worldwide suffered from dementia and that the annual cost of caring for these patients was over US\$600 billion.¹ By 2050, the WHO projects there will be more than 115 million people with dementia. Alzheimer's disease (AD), a grievous illness characterized by irreversible neurodegeneration, contributes to a majority of such cases. Despite its identification over a century ago, there is no known disease-modifying therapy, and the few available treatments provide only temporary symptomatic relief.² Currently in Phase III trials for the treatment of AD, verubecestat³ (MK-8931, **1**) is an inhibitor of β -secretase, an aspartic protease believed to be responsible for the cerebral deposition of the amyloid β peptides which accompany the presentation of AD.⁴

The principal challenge identified in our retrosynthetic analysis of **1** was the stereoselective formation of the central chiral tertiary carbamate (Figure 1). Far-reaching explorations into possible preparations of this key functional group identified an option that was viable for a commercial scale synthesis: the diastereoselective Mannich-type addition of a suitable methyl sulfonamide (**8**) to a chiral Ellman sulfinyl ketimine (**7**).⁵ After removal of both the

sulfonamide protecting group and the chiral auxiliary, intramolecular cyclization of the resulting diamine (**2**) with a source of cyanogen would provide the desired guanidine of **1**. We envisioned that the remaining portion of our target molecule could be built simply either by an amide coupling of 4-fluoropicolinic acid (**3**) with an aniline-containing partner (**5**) or by a transition-metal-catalyzed C–N coupling of 4-fluoropicolinamide (**4**) with an appropriate aryl bromide (**6**). All of these disconnections lead back to intermediates that are or can be readily prepared from commercially available materials. The challenge of how to efficiently synthesize **1**, then, was reduced to the questions of how to construct the secondary amide and how to best strategically order the remaining bond-forming steps.

The first-generation supply route to **1**, which was inspired heavily by the medicinal chemistry synthesis,⁶ has been used to support development from preclinical safety batches through to the ongoing clinical studies (Scheme 1). It relied on the amide coupling of **3** with aniline **13**, but since the acidic N–H protons of either the aniline or the resulting secondary amide would interfere with the highly basic conditions necessary for the desired Mannich-type addition, that functional group was masked as the corresponding nitro group in ketimine **9**. With those strategic decisions made, the synthesis proceeded in a relatively straightforward manner. Addition of lithiated **8** to **9** gave the chiral tertiary carbamate-containing **10**, which could be deprotected in situ and then upgraded in stereochemical purity to mandelate salt **11**. Subsequent cyclization with cyanogen bromide to **12** and protection of the newly formed guanidine provided an intermediate at which the desired aniline-containing compound (**13**) could be unveiled through hydrogenation. As planned, an amide coupling of **3** using propylphosphonic

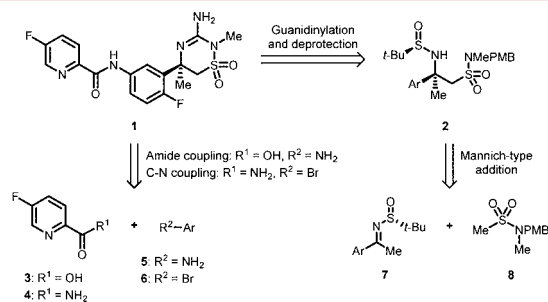
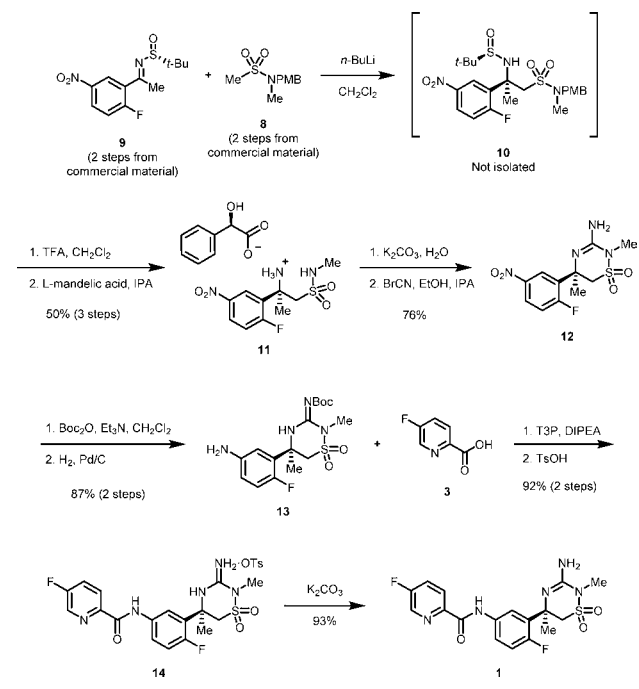


Figure 1. Retrosynthetic analysis of verubecestat (**1**).

Received: June 20, 2016

Published: November 4, 2016

Scheme 1. First-Generation Supply Route to Verubecestat



anhydride (T3P) to **14** and deprotection of the guanidine furnished **1**. Despite the ability of this robust synthesis to provide requisite quantities of active pharmaceutical ingredient (API), several aspects of the sequence drew our attention as areas that could be improved. Its reliance on both a *tert*-butoxycarbonyl group to mask the guanidine core and a chiral salt upgrade contributes to a linear synthetic sequence of 12 steps, a length that results in an only modest overall process efficiency. In addition, the highly exothermic heterogeneous aryl nitro reduction that generates aniline **13** is accompanied by the formation of many impurities that necessitate serial recrystallizations to meet quality specifications. Several transformations also employ the carcinogenic solvent dichloromethane, which we believed could be eliminated from the synthesis altogether. Finally, we expected that the yield of several steps could be significantly improved with further process optimization.

The lynchpin of our revised synthetic route to **1** was replacing the amide coupling with a transition metal-catalyzed C–N coupling (**4** + **6**, Figure 1). This would permit the aryl partner to be substituted with a bromide instead of a nitro group, a functional handle that we anticipated would not only be inert to the other planned transformations but also obviate the problematic hydrogenation. We hypothesized that there were at least three reasonable synthetic intermediates at which such a C–N coupling could be performed, and so we prepared each and evaluated them by high-throughput screening (HTS) of catalysts and reaction conditions (Figure 2). The most advanced intermediate considered, guanidine **17**, could be engaged productively in C–N bond formation, but the basicity of the guanidine moiety proved challenging for most catalyst systems, and only a few palladium-based methods (most notably Pd(OAc)₂ in combination with the ligand *t*-BuBrettPhos⁷) showed promise. Preliminary scale-up experiments, however, revealed that these options need significant catalyst loadings, a requirement that we expected would not ultimately be economically viable. We found that the next most advanced intermediate, diamine **16**, was susceptible under relevant catalytic conditions to competitive intramolecular

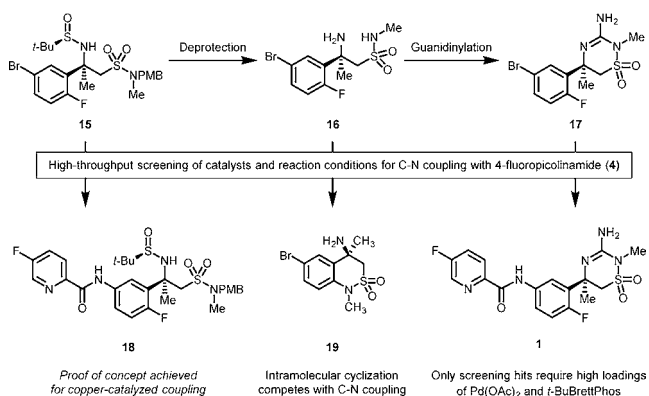
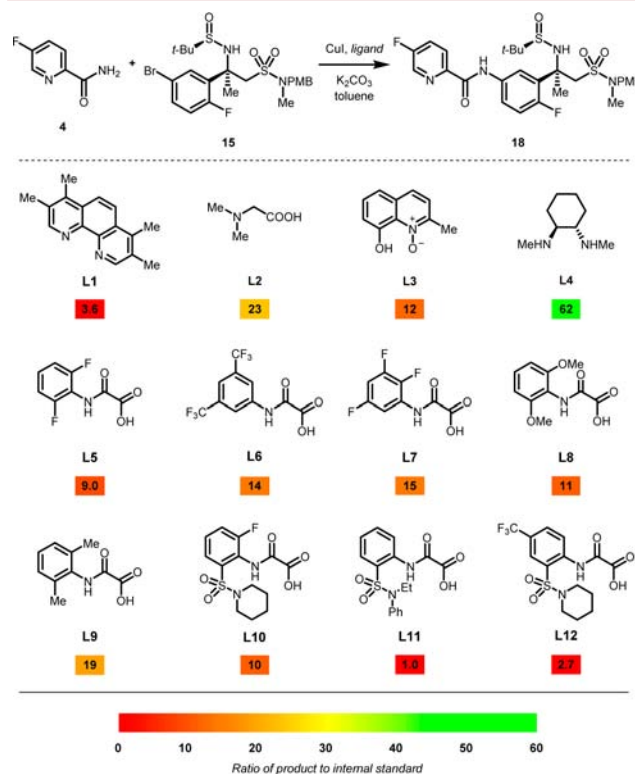


Figure 2. C–N coupling options evaluated by high-throughput screening of catalysts and reaction conditions.

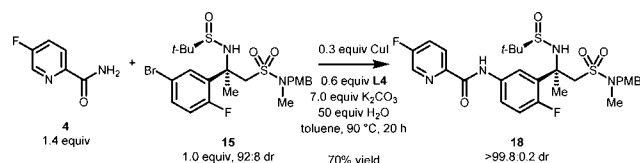
S_NAr-like cyclization of the unprotected methyl sulfonamide onto the pendant aryl fluoride. To our delight, HTS of reactions with bis-protected aryl bromide **15**, one synthetic operation removed from **16**, revealed many copper-based catalysts⁸ that could support the desired coupling.

We next optimized conditions for this reaction through a series of high-throughput experiments designed to assess each of the reaction parameters (e.g., copper source, ligand, base, solvent, and temperature). The copper salt precatalyst choice was largely inconsequential, but of the many ligands evaluated, 1,2-diamines provided the highest levels of reactivity (Figure 3). In particular, *trans*-*N,N'*-dimethylcyclohexane-1,2-diamine (**L4**) was differential, as it did not undergo appreciable levels of coupling with **15** itself under the reaction conditions, a side process that was observed with less sterically demanding 1,2-diamines (e.g., *N,N'*-

Figure 3. Selected C–N coupling ligand optimization results. (a) Results given as a ratio of product (**18**) to an internal standard as determined by UPLC analysis.

dimethylethylenediamine). The major undesired reaction pathway in this coupling is protodehalogenation of **15**; the choice of solvent in this regard was critical. Toluene was superior to many other high-boiling solvents (e.g., DMSO, DMF, DMAc, NMP, dioxane, *t*-AmOH) in suppressing the formation of des-bromo **15**, as was limiting the amount of moisture present in the reaction. For example, with 100 equiv of water present, 14.7% of des-bromo **15** was observed relative to **18**. Water could not be excluded, however, as it was needed to partially solubilize the base of choice, potassium carbonate. Ultimately, we established that 50 equiv of water provided the best balance between maximizing reactivity and minimizing protodehalogenation. Under the optimized conditions, C–N coupling product **18** was obtained in 80% assay yield and 70% isolated yield after crystallization (Scheme 2).

Scheme 2. Optimized Cu-Catalyzed C–N Coupling of **4** and **15**



Crucially, this isolation provides the pivotal stereochemical upgrade in the entire synthesis, as **18** is the only intermediate in which the *tert*-butylsulfonamide protecting group offers the opportunity to separate diastereomeric products. Crystallization of **18** from a solution of isopropyl alcohol and water upgrades the 92:8 ratio of diastereomers typically obtained in the Mannich-type addition to >99.8:0.2. The success of this isolation obviates the need to upgrade the stereochemical purity of an intermediate via the formation of a chiral salt, as was necessary in the first generation synthesis of **1**, effectively shaving two steps (i.e., forming and breaking the salt) off the longest linear sequence.

In the first-generation synthesis of **1** (Scheme 1), while the formation of ketimine **9** from 2-fluoro-5-nitroacetophenone and (*R*)-*tert*-butanesulfonamide (**21**) proceeded smoothly in >98% conversion, only a 67% yield of **9** was obtained. This is because the addition of water at the end of the reaction to begin the workup precipitates a superstoichiometric amount of titanium oxide, which requires a carbon treatment and multiple filter agent-assisted centrifuge filtrations, operations that result in significant product losses. Since titanium ethoxide appeared to be the singular cost-effective reagent available for this transformation and the analogous reaction with 2-fluoro-5-bromoacetophenone (**20**) achieved high conversion, our efforts focused on improving the workup and isolation process. The key breakthrough which enabled the isolation of sulfinyl ketimine **22** in higher yield and purity than that obtained when preparing **9** was the use of a 20 mol % aqueous solution of potassium glycolate. This salt solution efficiently chelates titanium alkoxides and oxides without any concomitant precipitation, allowing the various inorganic reaction byproducts to be simply washed away from the organics. With no amorphous solids to tediously filter,⁹ the desired product is obtained in 85% yield (Scheme 3).¹⁰

We were gratified to see that sulfinyl ketimine **21** readily underwent Mannich-type addition with deprotonated sulfonamide **8** to form the desired aryl bromide **15** in good yield and with high diastereoselectivity (Scheme 3). Importantly, the dichloromethane previously employed to conduct the analogous preparation of **10** could be replaced with THF with no deleterious impact on the reaction performance. Although **8** is significantly less soluble in THF than in dichloromethane and consequently

Scheme 3. Synthesis of Aryl Bromide **15**

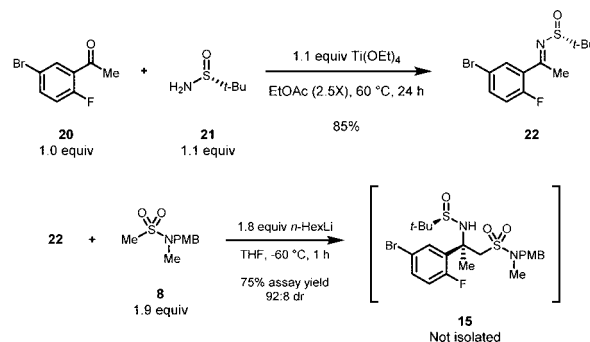


Table 1. Effect of Solvent on a Bis-deprotection Reaction^a

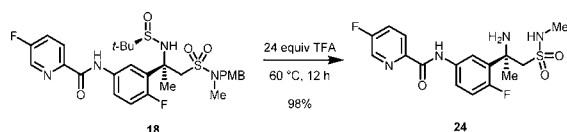
entry	solvent	23:16
1	CH ₂ Cl ₂	4:96
2	THF	100:0
3	IPAc	90:10
4	DMAc	92:8
5	NMP	91:9
6	CPME	98:2
7	MeCN	44:56
8	MTBE	94:6
9	<i>i</i> -PrOH	94:6
10	toluene	0:100

^aThe ratio of **23**:**16** was measured by HPLC analysis of the crude reaction mixture. In all cases, full conversion of **15** was observed.

reaches supersaturation at cryogenic temperatures, the corresponding organolithium species is highly soluble and, once prepared at –20 °C, can be brought without event to –60 °C for the desired reaction. These two qualities provided for significantly safer reagent handling and waste disposition at plant scale. Aryl bromide **15** is not a highly crystalline solid and so was carried forward in the synthesis as a solution.

The previous route to **1** includes an efficient trifluoroacetic acid mediated bis-deprotection of **10** (Scheme 1), and so we started our studies on the bis-deprotection of C–N coupling product **18** with the previously developed chemistry. Since replacement of dichloromethane with a greener alternative was the first priority, our attention turned to the choice of solvent. Of the two protecting groups, the *p*-methoxybenzyl is by far the harder to remove, and in a closely related study on the bis-deprotection of **15** to **16**, we were surprised to find that in many solvents the reaction stalls at the partially deprotected **23** (Table 1). After 18 h at 60 °C, a reaction in dichloromethane provides a 4:96 ratio of **23**:**16** (entry 1), but in many other common solvents (entries 2–9), conversion to the desired product is much lower. The use of toluene, however, provides exclusively **16** (entry 10). Unfortunately, under these conditions, crude reaction samples were contaminated with nonpolar polymeric material, presumably from copolymerization of toluene with the *p*-methoxybenzyl cation generated under these strongly acidic conditions. The employment of neat trifluoroacetic acid, however, largely suppresses the formation of such polymers, and with 3 volumes of acid (24 equiv relative to **18**) to control the large adiabatic temperature rise that accompanies this

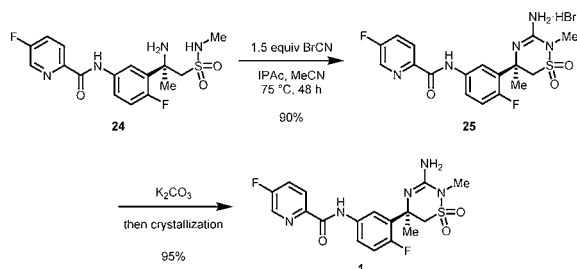
Scheme 4. Bis-deprotection of 18 with Trifluoroacetic Acid



reaction, the desired bis-deprotection of 18 delivers 24 in high yield (Scheme 4).

The guanidinylation of 11 to 12 with cyanogen bromide proceeded in only moderate yield (Scheme 1), in part because the reaction requires 48 h at 85 °C to reach high levels of conversion. During this time, guanidine 12 that is formed slowly degrades in solution, reducing the yield obtained after isolation. We explored other reagents for the guanidinylation of 24 (e.g., 1-cyano-4-methoxybenzene, *N*-cyanoimido-*S,S*-dimethyldithiocarbonate, and *S*-methylisothiourea) without success, and we could not significantly improve the rate of reaction through higher temperatures and pressures. However, we serendipitously discovered as part of a solvent screen that if the process was conducted in a mixture of isopropyl acetate and acetonitrile the HBr salt (25) of 1 spontaneously crystallized (Scheme 5). This

Scheme 5. Synthesis of Verubecestat (1) from 24



crucial observation provided three advantages over the previous chemistry. First, it allowed for the isolation of 25 simply by a filtration of the crude reaction stream, obviating the need to perform an aqueous workup or separate crystallization unit operation. Second, 25 came out of solution in >99% purity, a phenomenon that enabled a robust downstream isolation of 1 suitable for clinical studies. Third, the reactive crystallization of 25 phase separates the product from the remaining reaction components, conferring a remarkable degree of stability over the prolonged reaction times. This results in a significantly higher yield of 25 than what was correspondingly obtained in the first-generation synthesis. Free basing 25 with potassium carbonate and then crystallization of the API from ethyl acetate and heptane provides 1 in a purity suitable for clinical studies and manufacture.

The sum of this work represents a viable commercial synthesis of verubecestat (1). The overall yield of 37% through the longest linear sequence is over three times the 13% yield of the first-generation route. This was achieved not only by redesigning the route to take advantage of a key C–N coupling but also minimizing protecting group manipulations and avoiding a chiral salt upgrade. Further improvements were realized by developing more robust isolations and purifications for several transformations (such as the workup of sulfinyl ketimine 22 and the guanidinylation of 24). This dramatic increase in efficiency across the board has reduced the synthesis cost of 1 by more than half and enabled a much greener production going forward, as the waste generated in the second-generation synthesis is over 70% less than the first.

■ ASSOCIATED CONTENT

§ Supporting Information

The Supporting Information is available free of charge on the ACS Publications website at DOI: 10.1021/acs.orglett.6b01793.

Experimental procedures, compound characterization data, and NMR spectra (PDF)

■ AUTHOR INFORMATION

Corresponding Authors

*E-mail: david.thaisrivongs@merck.com.

*E-mail: steven.miller@merck.com.

Notes

The authors declare no competing financial interest.

■ ACKNOWLEDGMENTS

We thank Xiaodong Bu, Li Zhang, and Daniel Zewge for analytical chemistry support and Paul Devine and Louis-Charles Campeau for helpful discussions. All are members of Process Research and Development, Merck Research Laboratories.

■ REFERENCES

- (1) Duthey, B. Background Paper 6.11 Alzheimer Disease and other Dementias. Report for the European Commission by the World Health Organization; WHO, Feb 20, 2013.
- (2) Alzheimer's Disease Medications Fact Sheet. <https://www.nia.nih.gov/alzheimers/publication/alzheimers-disease-medications-fact-sheet> (accessed Jul 11, 2016).
- (3) (a) Scott, J. D.; Stamford, A. W.; Gilbert, E. J.; Cumming, J. N.; Iserloh, U.; Misiaszek, J. A.; Li, G. PCT Int. Appl. WO 2011/044181 A1, PCT/US2010/051553, 2011. (b) Kennedy, M. E.; Stamford, A. W.; Chen, X.; Cox, K.; Cumming, J. N.; Dockendorf, M. F.; Egan, M.; Ersehefsky, L.; Hodgson, R. A.; Hyde, L. A.; Jhee, S.; Kleijn, H. J.; Kuvelkar, R.; Li, W.; Mattson, B. A.; Mei, H.; Palcza, J.; Scott, J. D.; Tanen, M.; Troyer, M. D.; Tseng, J. L.; Stone, J. A.; Parker, E. M.; Forman, M. S. *Sci. Transl. Med.* **2016**, 8, 363ra150.
- (4) Vassar, R.; Bennett, B. D.; Babu-Khan, S. B.; Kahn, S.; Mendiaz, E. A.; Denis, P.; Teplow, D. B.; Ross, S.; Amarante, P.; Lealoff, R.; Luo, Y.; Fisher, S.; Fuller, J.; Edenson, S.; Lile, J.; Jarosinski, M. A.; Biere, A. L.; Curran, E.; Burgess, T.; Louis, J.-C.; Collins, F.; Treanor, J.; Rogers, G.; Citron, M. *Science* **1999**, 286, 735.
- (5) (a) Cogan, D. A.; Ellman, J. A. *J. Am. Chem. Soc.* **1999**, 121, 268. (b) Robak, M. T.; Herbage, M. A.; Ellman, J. A. *Chem. Rev.* **2010**, 110, 3600.
- (6) Scott, J. D.; Li, S. W.; Brunskill, A. P. J.; Chen, X.; Cox, K.; Cumming, J. N.; Forman, M.; Gilbert, E. J.; Hodgson, R. A.; Hyde, L. A.; Jiang, Q.; Iserloh, U.; Kazakevich, I.; Kuvelkar, R.; Mei, H.; Meredith, J.; Misiaszek, J.; Orth, P.; Rossiter, L. M.; Slater, M.; Stone, J.; Strickland, C.; Voigt, J. H.; Wang, G.; Wang, H.; Wu, Y.; Greenlee, W. J.; Parker, E. M.; Kennedy, M. E.; Stamford, A. W. *J. Med. Chem.* **2016**, DOI: 10.1021/acs.jmedchem.6b00307.
- (7) Fors, B. P.; Watson, D. W.; Biscoe, M. R.; Buchwald, S. L. *J. Am. Chem. Soc.* **2008**, 130, 13552.
- (8) (a) Klapars, A.; Antilla, J. C.; Huang, X.; Buchwald, S. L. *J. Am. Chem. Soc.* **2001**, 123, 7727. (b) Klapars, A.; Huang, X.; Buchwald, S. L. *J. Am. Chem. Soc.* **2002**, 124, 7421.
- (9) For a related strategy employing an EDTE-chelate of soluble titanium, see: Reeves, J. T.; Tan, Z.; Han, Z. S.; Li, G.; Zhang, Y.; Xu, Y.; Reeves, D. C.; Gonnella, N. C.; Ma, S.; Lee, H.; Lu, B. Z.; Senanayake, C. H. *Angew. Chem., Int. Ed.* **2012**, 51, 1400.
- (10) A recent report demonstrates that the use of $\text{B}(\text{OCH}_2\text{CF}_3)_3$ instead of $\text{Ti}(\text{OEt})_4$ to form sulfinyl ketimines simplifies the workup protocol: Reeves, J. T.; Visco, M. D.; Marsini, M. A.; Grinberg, N.; Busacca, C. A.; Mattson, A. E.; Senanayake, C. H. *Org. Lett.* **2015**, 17, 2442.